The Hydrosphere State (HYDROS) Mission: An Earth System Pathfinder for Global Mapping of Soil Moisture and Land Freeze/Thaw

Dara Entekhabi, Eni Njoku, Paul Houser, M. Spencer, T. Doiron, J. Smith, R. Girard, S. Belair, W. Crow, T. Jackson, Y. Kerr, J. Kimball, R. Koster, K. McDonald, P. O'Neill, T. Pultz, S. Running, J.C. Shi, E. Wood, J. van Zyl

Abstract— **The Hydrosphere State Mission (HYDROS) is a pathfinder mission in the National Aeronautics and Space Administration (NASA) Earth System Pathfinder Program (ESSP). The objective of the mission is to provide exploratory measurements that constitute the first global scale measurement of Earth's soil moisture and land surface freeze/thaw conditions. The mission builds on the heritage of ground-based and airborne passive and active low-frequency microwave measurements that have demonstrated and validated the effectiveness of the measurements and associated algorithms for estimating the amount and phase (frozen or thawed) of surface soil moisture. The mission data will enable advances in weather and climate prediction and in mapping processes that link the water, energy and carbon cycles. The HYDROS instrument is a combined radar and radiometer system operating at 1.26 GHz (with VV, HH, and HV polarizations) and 1.41 GHz (with H, V, and U polarizations) respectively. The radar and the radiometer share the aperture of a 6-meter antenna pointing at 35 degrees with respect to nadir. The lightweight deployable mesh antenna is rotated at 14.6 rpm to provide a constant look-angle scan across a swath width of 1000 km. The wide swath provides a global coverage of the Earth in 2 to 3 days with a temporal sampling less than 2 days at latitudes above 50N. The radiometer measurements allow retrieval of soil moisture in diverse (non-forested) landscapes with a resolution of 40 km. The radar measurements allow the retrieval of soil moisture at relatively high resolution (3 to 10 km). The mission includes combined radar/radiometer data products that will use the synergy of the two sensors to deliver enhanced quality soil moisture estimates. In this paper the science requirements and their traceability to the instrument design are outlined. A review of the underlying measurement physics and key instrument performance parameters are also presented.**

Keywords— ***Index Terms:*** **Soil Moisture, Land Freeze/Thaw, Microwave Remote Sensing, Satellites**

I. Introduction

The Hydrosphere State (HYDROS) mission will use a combined passive/active low-frequency (L-band) microwave instrument to measure the land hydrosphere state globally from space. HYDROS will provide measurements of surface soil moisture (0 to 5 cm depth) and land freeze/thaw state over a wide 1000 km swath with a global revisit of 2 to 3 days (1 to 2 days above 50 degree latitude). Over 70% of the swath the radar resolution is better than 3 km. The radiometer resolution is about 40 km. Measurements from these sensors are combined to produce a global 10 km soil moisture data product.

[0]Manuscript received xxxx; revised yyyy.

The corresponding author D. Entekhabi is with Department of Civil and Environmental Engineering, Massachusetts Institute of Technology, Cambridge, MA 02139.

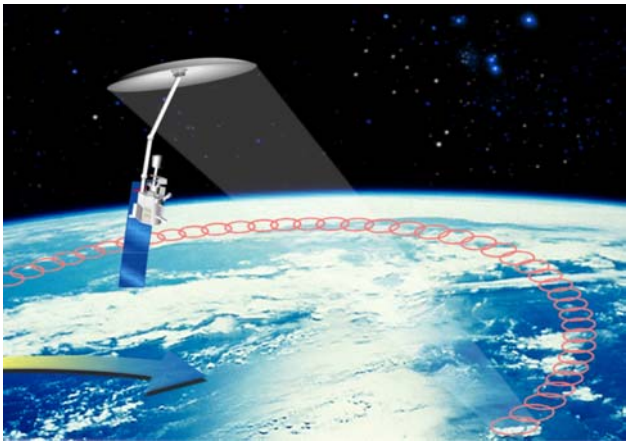

Fig. 1. The Hydrosphere State (HYDROS) Mission

The radar and the radiometer share the aperture of a large (6-meter) but light-weight deployable mesh reflector. The reflector rotates to make conical scans over a wide swath (~1000 km). In this way HYDROS will produce global mapping with high revisit (see Figure 1).

The HYDROS mission has been selected as a NASA Earth System Science Pathfinder (ESSP). In this paper the scientific bases and the measurement approach for the HYDROS mission is described. In Section 2 the scientific motivation for making the measurements is presented. The science and application requirements for measurements are defined and the underlying physics of the measurements are also reviewed. The measurement requirements and underlying physics are traced to the instrument concept outlined in Section 3. In Section 4 the retrieval algorithms and data products are reviewed. The status of the HYDROS mission and time-line for implementation are presented in the concluding Section 5.

II. Science and Application Requirements for Soil Moisture and Land Freeze/Thaw Measurements

Measurements of soil moisture and its freeze/thaw state are critical components in approaching high-priority questions in Earth system science today [1]. These include key

questions about the water and energy cycle as well as the carbon cycle. Soil moisture is often the limiting factor in evaporation from the landscape. Plants transpire water by extracting moisture from the surface soil and throughout the root-zone. Evaporation from soil surface and transpiration through vegetation is also dependent on the availability of moisture. Since large amounts of energy are required to vaporize water, soil control on evaporation also has a significant impact on the energy cycle. Soil moisture and its freeze/thaw state are also key determinants of the global carbon cycle. Carbon uptake and release in boreal landscapes is one of the major source of uncertainty in assessing the carbon budget of the Earth system (the so-called 'missing carbon sink'). HYDROS is an exploratory mission to demonstrate that global measurements of soil moisture and its freeze/thaw state can be made with the precision, spatial resolution, and temporal frequency to address critical science questions in water, energy, and carbon cycles.

A. Key Scientific Applications and Their Data Requirements

Global change projections on decadal and century time scales are built on foundations of conceptual understanding and modeling. However, there is significant uncertainty associated with the model-based projections is largely influenced by the uncertainty in the representation of land-surface processes. Whereas the uncertainty of different model projections of global change in terms of variables such as temperature may have lessened over the last few years, simulations of surface hydrological processes are at odds among climate models [2]. An effective way to diagnose errors in surface hydrologic processes in climate models is to examine how they simulate the partitioning of atmospheric forcing (available energy into sensible and latent heat flux and precipitation into runoff and infiltration) as a function of regional soil moisture[3][4].

Figure 2 shows the control of soil moisture over surface evaporation at a specific site [5]. The fractional surface evaporation (with respect to its upper limit, potential evaporation) is shown to depend strongly on surface soil moisture, here as measured by an L-band radiometer (a ground-based prototype of the HYDROS instrument). The correct model representations of this relationship and the corresponding relationship for runoff ratio (ratio of runoff to precipitation), are critical for climate and global change studies. HYDROS measurements provide the required missing soil moisture element for performing such stringent tests of land surface models.

Measurements of soil moisture and its freeze/thaw state are of practical importance to weather and climate prediction Numerous sensitivity studies using surrogate soil moisture data have shown that simulations forced with fixed or incorrect soil moisture are not capable of reproducing the observed climate with fidelity. Improvements in shorter-term weather forecasting have come more from the introduction of new data types and their modeling than from incremental increases in the sampling of existing data

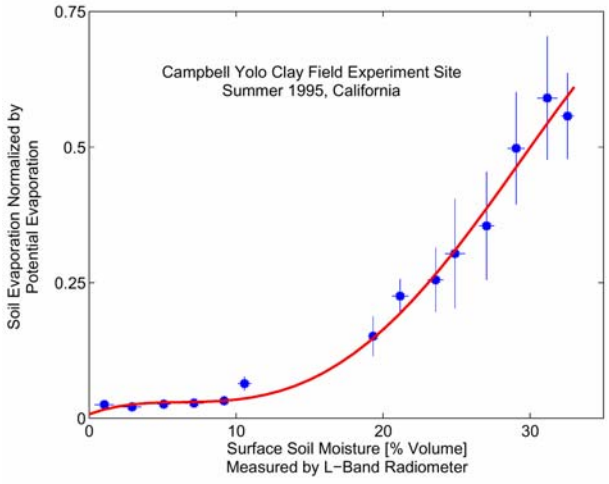

Fig. 2. A ground-based L-band radiometer is used to make the soil moisture field measurements to estimate the surface control on evaporation (Cahill, 1999). Red-line is a fit through the discrete estimates. Global HYDROS soil moisture measurements, together with meteorological and hydrological data, will allow for the first time a quantification of influential processes such as this across diverse climatic and seasonal regimes.

types. At the National Center for Environmental Prediction (NCEP), simply improving the parameterization of surface-atmosphere exchanges brought the same gains in forecast accuracy of 3-day-ahead precipitation as the doubling of atmospheric model resolution [1]. At the European Center for Medium-range Weather Forecasting (ECMWF), improvements in the treatment of freeze/thaw and albedo dynamics resulted in the removal of a 5° C bias in 5-day surface air temperature forecasts[6]. An important improvement, for boundary-layer evolution and precipitation bias, was also noticed at the Canadian Meteorological Centre when they implemented a new land surface modeling and assimilation system in their short-range regional weather forecast model [7].

For soil moisture, evolving weather systems are impacted by surface characteristics through atmospheric boundary layer (ABL) coupling. The ABL integrates and responds to surface fluxes on a ~10 km or hydrometeorological scale [8]. At larger scales, regional variations in surface states affect the intraseasonal climate through the modulation of populations of weather events. Examples are regional moisture recycling and standing atmospheric pressure ridge/trough formation that require knowledge of boundary characteristics resolved at the ~40-km or better hydroclimatological scale. The temporal sampling requirements for surface soil moisture follow from the time scales of surface wetting and drying. Capturing the impacts of storm/interstorm sequences com-bined with the inertia of surface storage requires a revisit of ~3 days. The desired accuracy for soil moisture is +/- 4% volumetric (one standard deviation), which provides at least 5 levels of moisture discrimination between dry and saturated and allows estimation of surface fluxes to within in situ observational error. The moisture estimate is required over a depth that is no shallower than

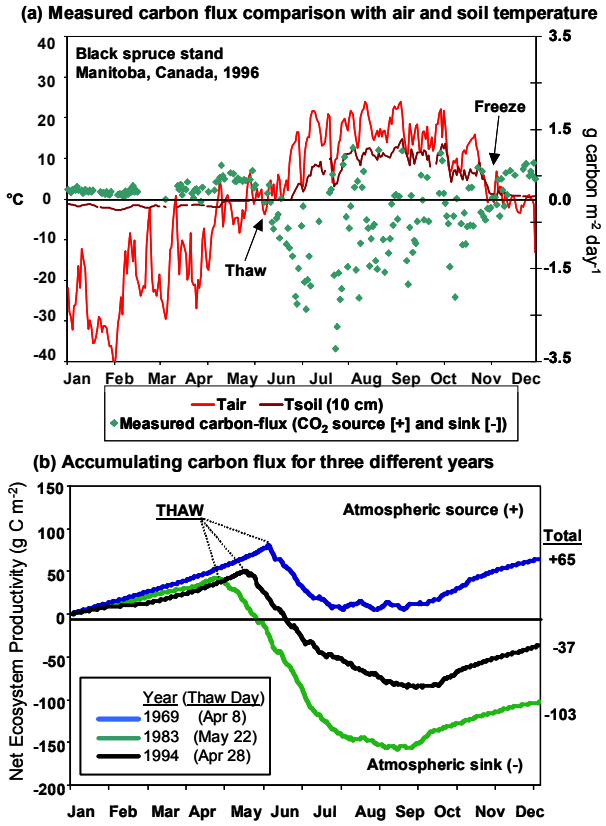

Fig. 3. The top panel (a) compares tower eddy-flux measurements of CO2 exchange with air and soil temperature at a field site. (b) Shows the simulated accumulation of net carbon flux at the site for years having early, average, and late spring thaw (Frolking et al., 1996). Depending on the timing of the thaw date (in lower panel legend), the site can be a net annual source or sink of atmospheric carbon. HYDROS will provide global observations of seasonal freeze/thaw cycles.

2 to 5 cm so that moisture beneath the surface skin layer is detected and linkage to models for data assimilation can be reliably accomplished to extrapolate surface soil moisture to the root zone. The science requirements for surface soil moisture volumetric content are summarized in the first column of Table 1.

One of the largest unknowns in understanding the global carbon cycle and associated linkages with the atmosphere is the nature and distribution of the so-called "missing carbon sink." This sink is thought to exist somewhere within the terrestrial mid- to high-latitudes and may be due to carbon sequestration in forests. In these land eco-systems, the state transition between frozen and thawed conditions affects a number of processes that cycle between winter (dormant) and summer (active) states. Timing of spring thaw governs the length of the growing season and is strongly linked to the amount of carbon sequestered annually by vegetation (Figure 3).

In boreal ecosystems, earlier spring thaws lead to significant increases in net carbon uptake [9][10]. Figure 3 shows that at the BOREAS experiment site the ecosystem transition from a carbon source to a sink is coincident with thaw. The timing of this transition is key to quantifying boreal landscape carbon exchange with the atmosphere. Ecosystem process simula-tions over multiple years for boreal forest stands show 6- to 7-week ranges in the timing of soil thaw [11]. These variations result in substantial effects on eco-system carbon productivity; they can deter-mine the magnitude of annual carbon exchange and whether the ecosystem is altogether a net source or sink of atmospheric carbon (Figure 3).

Instrumented temperature records show that the Northern latitudes are particularly vulnerable to warming trends [12]. These trends are also apparent in other independent observations including snow cover extent, river ice breakup, vegetation green-up, and snowmelt/streamflow (e.g., [13]). Projections of future climate show global warming trends will be significantly more pronounced in northern latitudes. Large changes in land-atmosphere carbon exchange will take place if the length of the growing season increases. Moreover, the loss of hydrographic-monitoring capabilities across the pan-Arctic is particularly acute and may inter-fere with understanding of high-latitude and global environmental change [14].

HYDROS freeze/thaw state measurements will be a magnifying lens for assessing how ecosystems respond to and affect global environmental change. Such data sets will improve regional mapping and prediction of boreal-arctic ecosystem processes and associated carbon dynamics and are considered critical to observational support for pan-Arctic monitoring and synthesis studies.

Freeze/thaw dynamics in boreal latitudes cover an entirely different range of scales than those discussed for soil moisture earlier. The heterogeneity of landscape features results in small-scale variations in the freeze/thaw field. These variations are strongly linked to land surface features (soil texture, land cover, slope, aspect, snow cover) and microclimate environment. These features exhibit a high degree of spatial heterogeneity in northern latitudes. As a result, freeze/thaw state is also spatially complex and mapping at ~3 km or less is required. [15][13][16]. Temporal sampling requirements for freeze/thaw detection follow directly from primary applications. For example, resolving the carbon source/sink dynamics of boreal ecosystems requires measurements that can resolve the temporal dynamics of net ecosys-tem exchange to within $\pm$ 0.05 tons C ha^{-1} over a 100-day growing season. Given reported average daily fluxes, a measurement fidelity of 2 days is required for linking the dynamic coevolution of surface state and water, energy, and carbon fluxes. These science requirements for freeze/thaw measurements are summarized in the first column of Table 1. Together with those discussed earlier for soil moisture, they represent the science requirements for the HYDROS mission. In the following section the underlying physics of the measurements needed to meet the science objectives are described. The instrument functional requirements follow from the science requirements and the understanding of the underlying physics of measurements (See Section 3).

B. Underlying Physics of the Measurements

B.1 Surface Soil Moisture in Non-Forested Landscapes

The variability of soil moisture and its impact on global weather and climate are greatest in non-forested regions at the transition zones between water-limiting and radiation-limiting evaporation regimes. Measurements of soil moisture in these areas (estimated to encompass approximately 65% of the global land surface) are, therefore, a main focus of the HYDROS mission.

Soil moisture will be estimated using HYDROS radiometer and radar measurements in combination, taking advantage of the simultaneous, coincident, and complementary nature of the measurements. Both radiometer and radar measurements have been shown to be sensitive to soil moisture and can be used independently to estimate soil moisture. There can be upto 100 K difference in radiobrightness at L-band between dry and saturated soils[17]. There is also considerable sensitivity in backscatter at L-band due to soil moisture variations. Between dry and saturated soils and between thawed and frozen soils the difference in backscatter can reach up to 10 dB. The sensitivity to soil moisture is however strongly affected by confounding factors such as vegetation and surface roughness. Under vegetated conditions, radiometric retrieval algorithms currently provide more accurate soil moisture estimates than radar algorithms. The radar measurements, on the other hand, have a higher spatial resolution and provide sub-pixel roughness and vegetation information within the lower-resolution radiometer footprint. Hence, the combination of simultaneous radar and radiometer data can enhance both the resolution capability and accuracy of soil moisture estimates.

Soil and canopy temperature, soil roughness, surface topography, and soil texture also affect the measurements. At dawn the soil surface and canopy temperatures and the soil subsurface moisture and temperature profiles are approximately uniform and Faraday rotation and scintillation effects are small (for both active and passive measurements), providing optimal retrieval conditions. Contributions from clouds and atmospheric gaseous absorption and emission are minimal at L-band. Soil roughness, topography, and vegetation conditions at the HYDROS footprint scale vary slowly relative to the soil moisture dynamics in their effects on the sensor measurements. Hence, soil moisture can be derived using both relative change and absolute estimation approaches.

The primary relationships between surface features and observed brightness temperatures T_{B_p} at polarization p (V or H) can be expressed as:

$$\begin{aligned} T_{B_p} &= T_s\, e_p\, \exp\left(-\tau_c\right) + T_c\left(1-\omega\right) \\ &\quad \left[1-\exp\left(-\tau_c\right)\right]\left[1+r_p \exp\left(-\tau_c\right)\right] \end{aligned} \tag{1}$$

where T_s and T_c are the physical temperatures (K) of the soil and vegetation, τ_c is the vegetation opacity along the slant path, and r_p is the soil reflectivity (both at look angle θ). The reflectivity is related to the emissivity by $e_p = (1 - r_p)$. At L-band, vegetation is predominantly absorbing, with small single-scattering albedo [18]; for vegetation cover at several tens of km scale, the opacity can be considered to be azimuthally isotropic and unpolarized. The vegetation opacity is related to the columnar vegetation water content W_c (kg m^{-2}) by the relation:

$$\tau_c = b\, W_c \,/\, \cos\left(\theta\right) \tag{2}$$

where b is a coefficient that depends on vegetation type [19]. Both b and W_c can be estimated using ancillary data bases derived from satellites. If more refined information on phenological stage is available it may be possible improve the estimation of b. W_c can be estimated using vegetation indices [20]. These parameters might also be derived from higher frequency microwave observations from other satellites [21][22]. The surface reflectivity r_p is related to the soil dielectric constant ε by the Fresnel equations, with modifications for surface roughness [23]. Roughness influences the sensor response primarily through the RMS surface height, with horizontal correlation length as a secondary influence. The dielectric constant is related to the soil moisture content m_v (percent volumetric) using models derived from laboratory measurements, with a parametric dependence on soil texture [24][25].

For the radar, the total co-polarized backscatter from the surface is the sum of three components:

$$\sigma^t_{pp} = \sigma^s_{pp}\, \exp\left(-2\tau_c\right) + \sigma^{vol}_{pp} + \sigma^{int}_{pp} \tag{3}$$

The first term is the soil surface backscatter, σ^s_{pp}, modified by the two-way attenuation through a vegetation layer of opacity τ_c (along the slant path at look angle θ, and assumed unpolarized as for the passive case). The second and third terms represent, respectively, the backscatter from the vegetation volume, σ^{vol}_{pp}, and the interaction between the vegetation and soil surface, σ^{int}_{pp} [26]. For bare or low-vegetated conditions, the σ^s_{pp} contribution dominates the received signal and is influenced primarily by the soil moisture and RMS surface roughness. The backscatter dependence on vegetation characteristics is complex and is influenced (to a greater extent than the passive case) by the shapes, sizes, and orientations of the vegetation components.

Field experiment results show that L-band radiobrightness and backscatter measurements can be used in conjunction with (1) and (3) to estimate surface soil moisture. An example of such tests and comparison with ground-truth measurements show that the estimation RMSE is about 3% for radiometer and about 4% for radar over bare soil and low vegetation (Figure 4). Recent results from the SMEX02 field experiment have confirmed these findings.

B.2 Surface Freeze/Thaw in Boreal Landscapes

The capability of L-band radar measurements to detect freeze/thaw transitions in a robust way is demonstrated in Figure **??**. JERS-1 L-band imagery of forested and wetland regions in Alaska are used to examine the spatial heterogeneity of springtime thaw. The series of images shows

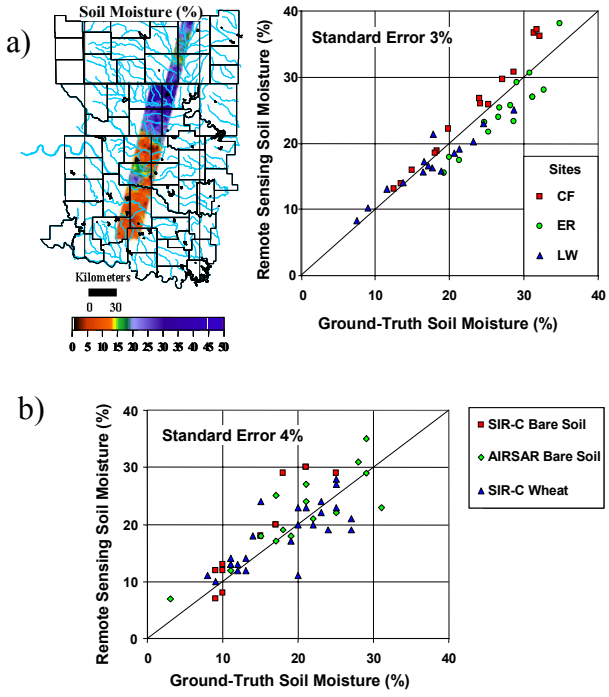

Fig. 4. HYDROS soil moisture algorithms are based on a heritage of experiments using ground-based, airborne and Shuttle instruments. (a) Soil moisture map and retrieval performance using airborne radiometer (ESTAR) measurements, and (b) Soil moisture retrieval performance using Airborne (AIRSAR) and Shuttle (SIR-C) radar measurements.

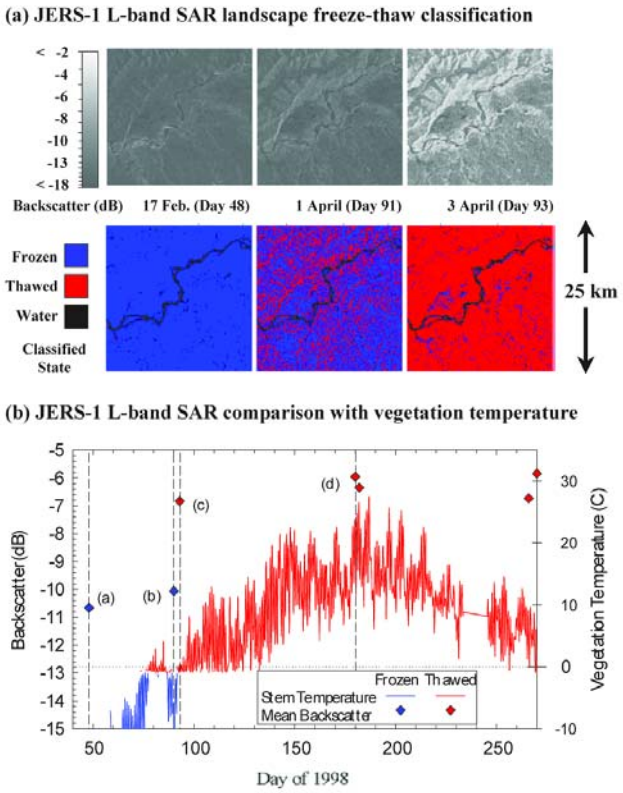

Fig. 5. The series of JERS L-band SAR images from central Alaska show the spring thaw transition. The lower panel (b) compares vegetation tissue temperature to backscatter. The HYDROS global mapping capability and high revisit will provide a 15- to 20-fold improvement in temporal discrimination of freeze/thaw state transitions across boreal latitudes.

the spatially complex nature of the springtime thaw transition. Freeze-thaw state in boreal regions has previously been mapped with spaceborne SARs and scatterometers (e.g.,[27][28][29][15]. Results demonstrate that these seasonal transitions are spatially heterogeneous and undergo several thaw and re-freeze cycles in a season. These characteristics underscore the need for mapping with combined high spatial resolution and high revisit [30]. L-band radar penetrates vegetation canopies more readily than shorter wavelength radars, providing more backscatter sensitivity to freeze/thaw state transitions throughout the soil-vegetation column. Also, the contrast in dielectric constant of frozen and thawed water is maximized at L-band relative to higher frequencies employed in most current and planned radar missions, yielding more backscatter sensitivity to dielectric variations in the soil and vegetation (see Figure 5).

III. Instrumentation and Mission Design

Table 1 summarizes the instrument functional requirements (second column) to meet the science requirements in the first column of the same table. The HYDROS instrument implementation approach is to develop radar and radiometer instrument components that share a lightweight, deployable mesh reflector antenna. Both active and passive measurements share a single single feedhorn which is used with the mesh reflector to form a beam offset from nadir by 35 deg and forming an incidence angle with the surface of 39.3 degrees (see Figure 1). This beam is rotated conically about the nadir axis to form a wide measurement swath. The reflector is composed of lightweight mesh material that can be stowed for launch . Once deployed it is supported by an extended boom. Two antenna rotation approaches are currently being considered in order to form the conical scan (see [31]). In one design the spin motor is placed between the top end of the boom and the antenna central hub to rotate only the 6 meter reflector; with the boom fixed relative to the spacecraft.

In an alternative design, the spin motor is placed down on the zenith deck of the spacecraft, the boom supports the reflector at the reflector rim, and the boom and reflector rotate together. In both designs, the feed assembly and electronics are fixed on the de-spun spacecraft, and there is therefore no electrical connection across the rotary interface (i.e., no RF rotary joint or slip rings). For either antenna architecture, the reflector will rotate about the nadir axis at 14.6 rpm to provide contiguous coverage over the 1000-km swath.

The instrument system will operate at 1.26 GHz and 1.29 GHz for the radar and 1.41 GHz for the radiometer and will

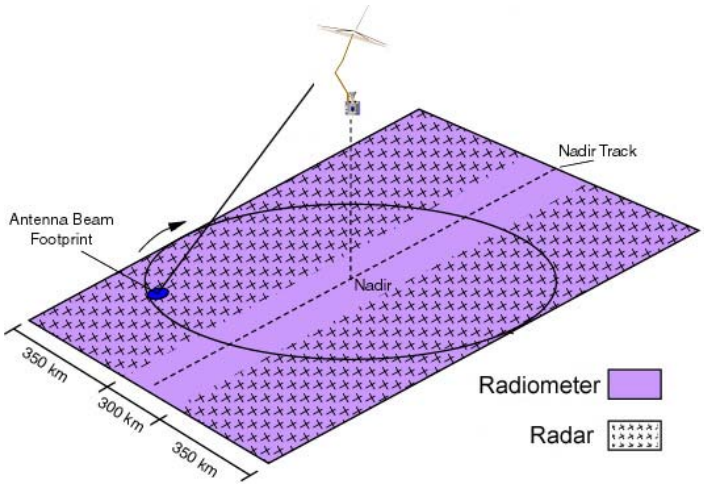

Fig. 6. The HYDROS instrument makes conical scan at constant incidence angle over a wide (~1000 km) swath.

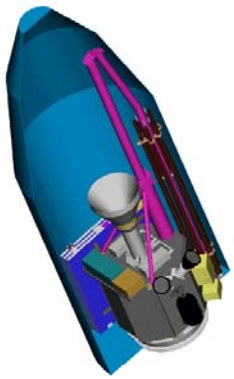

Fig. 7. Stowed reflector configuration.

make measurements at both horizontal and vertical linear polarizations with respect to the surface. Because the feed assembly is fixed relative to the spacecraft and the antenna reflector is rotating, the linear polarizations launched and or measured by the feed horn must somehow be rotated synchronously with the antenna in order to maintain the proper polarization geometry relative to the surface. In the current instrument architecture, this polarization rotation is accomplished with mechanically pin-polarizers inside the feed assembly. Techniques to rotate the radiometer polarizations without mechanical devices are also being considered. . The 6-m antenna diameter will produce a radiometer footprint of approximately 40 km (root ellipsoidal area), where the resolution is defined by the antenna 1-way 3-dB beam-width. Similarly, the radar 2-way 3-dB real aperture footprint will be 30 km. To obtain the required 3 km and 10 km resolution for the geophysical products, the radar will employ range and Doppler discrimination to sub-divide the antenna footprint. This is equivalent the application of unfocused synthetic aperture radar (SAR) techniques to the conically scanning radar case. Due to squint angle effects, the high-resolution products will not be obtained within the 300-km band of the swath centered on the nadir track (see Figure 6).

Measurement precision for a radiometer is proportional to the square root of the band-width and the measurement integration time (the time-bandwidth product). Given a reflector rotation rate of 14.6 rpm, the available integration time for each measurement is 42 ms. That value, however, will effectively be doubled when both fore and aft looking radiometer measurements are combined. Choosing a measurement bandwidth of 25 MHz and a system noise temperature of 590 K, the resulting precision is 0.4 K. The radiometer calibration stability is estimated to be 0.5 K. The root-sum square of 0.5 K and the 0.4 K precision specifications yield a total relative error of 0.64 K, satisfying the 1-K requirement of the soil moisture science objective.

There are two requirements placed on the radar relative error. The soil moisture measurement requirement places a 0.5 dB relative error requirement for both vertical and horizontal co-polarized backscattering coefficient measurements at 10 km resolution. The freeze/thaw state measurement places a 1 dB requirement on the relative error of each vertical and horizontal co-polarized backscatter measurement at 3 km resolution. The radar relative error depends on the signal-to-noise ratio (SNR) and the number of independent samples, or "looks", averaged in each measurement, as well as the relative calibration error. Looks will be obtained by averaging in both range and azimuth. The 1-MHz bandwidth will yield a ground range resolution of approximately 250 m and will result in a minimum of 12 looks in range for 3 km cells and 40 looks for 10 km cells.

As shown in Figure 8, the Doppler diversity will be maximized at a scan angle perpendicular to the platform velocity, leading to a single-look azimuth resolution of approximately 450 m. The single-look resolution will decrease as the scan angle approaches the platform velocity vector, reaching 1500 m at the inner swath edge (150-km cross-track). Table 2 provides a summary of the HYDROS instrument performance requirements.

The electronics subsystem is mounted on the zenith deck of the spacecraft, as close to the feed assembly as possible. A digital interface with the spacecraft C&DH is provided to transfer the radiometer science measurements and telemetry to the spacecraft recorder for transmission to the ground. The radiometer receives a timing signal to protect the receiver during radar transmit events. The radar RF electronics assembly, which creates the transmit pulses and amplifies and down-converts the return echoes, is also mounted on the zenith deck of the spacecraft. The radar digital electronics assembly, which governs the radar timing and performs digital processing on the return echoes, is located within the spacecraft avionics VME card cage, yielding a lower cost integrated design. The software necessary to command the radar timing and high-rate data collection is implemented on the spacecraft CPU. Radar data are transferred to spacecraft recorder via the high-speed interface within the VME cage.

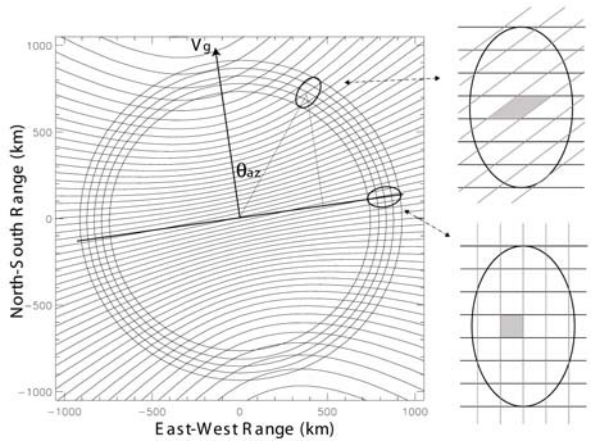

Fig. 8. Radar measurement geometry as a function of scan angle. The spacecraft velocity vector is shown as v_g. Also shown are the iso-Doppler contours that govern the radar azimuth resolution.

Table 2: Instrument Performance	
Radiometer	
Beamwidth (2-Way)	2.6° (1.9°)
Center Frequency	1.41 GHz
Footprint (Root Ellipsoid Area)	38 km
Channels	H, V, U
Bandwidth	25 MHz
Precision	0.40°K
Calibration Stability	0.50°K
Total Relative Error	0.64°K
Radar	
Transmit Frequencies	1.26 H,1.29 V GHz
Pulse Repetition Frequency	3.5 KHz
Pulse Length	15 μs
Maximum Exposure Length	32 ms
Transmit Bandwidth	1 MHz
Peak Transmit Power	500 W
Noise Equivalent	-39 dB

The selected spacecraft bus is a three-axis stabilized Spectrum Astro SA-200HP; this bus was selected for its high heritage and low cost. The HYDROS mission requirements result in a spacecraft design very similar to that used for the DoD Coriolis spacecraft, currently in flight. The spacecraft operates at 670 km altitude in a frozen, sun-synchronous, polar orbit with 6 am/pm equatorial crossings. The orbital altitude was chosen to provide whole Earth coverage and 3-day revisits. The orbit also provides adequate power margins with short eclipse periods. The equatorial crossing times were chosen to maximize valid science return as a) soil moisture/temperature profiles are uniform at dawn and b) ionosphere-caused Faraday rotation error is minimal at dawn.

IV. Retrieval Algorithms and Data Products

A. Retrieval Approaches

A.1 Brightness Temperature Soil Moisture Retrieval

Soil moisture will be estimated from HYDROS brightness temperature observations by inverting Equation (1). Ancillary data will be used to estimate the key unknown parameters: i.e., soil and vegetation temperatures (approximately equal to the surface air temperature at dawn), vegetation opacity, and surface roughness and soil texture. Estimates of the coefficients for surface roughness and the relations between vegetation indices and τ_c, have been derived from field experiments at L-band for a variety of conditions [18][32]. These coefficients are expected to be relatively time-invariant at the spatial scale of the HYDROS measurements (40 km) and will be validated and adjusted during the post-launch calibration/validation phase.

The baseline HYDROS radiometer retrieval algorithm uses the L-band H-pol channel. A two-channel (H–pol and V-pol) version of the algorithm using least-squares optimization will be evaluated during the pre-launch algorithm development phase as a means to potentially reduce the reliance on ancillary vegetation and surface temperature data. Such approaches have been investigated using simulated data [33][34] and are being further developed using data from SMEX02 and SMEX03 field experiments.

A.2 Radar Backscatter Soil Moisture Retrieval

Several algorithms have been developed to estimate soil moisture from bare soils [35][36][37]. A robust formulation uses the two co-polarized radar channels to separate the effects of soil moisture and surface roughness[36]. Linear combinations of the backscattering coefficients, σ^s_{vv} and σ^s_{hh}, are used to simultaneously estimate the dielectric constant, ε, and the RMS surface height, h. The soil moisture m_v is derived from ε using a dielectric model [24][25].

Radar retrievals of soil moisture using this method are expected to be accurate for regions of vegetation water content up to about 0.5 kg m^{-2} [26], significantly less than for the passive case. A radar-derived vegetation index (RVI) based on the $\sigma^t_{hv}/\sigma^t_{vv}$ ratio is used to screen out higher-vegetated areas [36]. Methods for estimating biomass and vegetation water content have been explored for higher vegetation levels using air-borne and spaceborne SAR data [38][39][40][41]. Radar measurements, especially the cross-polarized backscatter σ^t_{hv}, are sensitive to vegetation biomass and canopy characteristics. However, the backscatter dependence on vegetation characteristics is complex; quantitative algorithms for soil moisture estimation in high biomass regions are the subject of continuing research.

To extend the radar-based soil moisture retrieval capability to vegetation densities above ~0.5 kg m^{-2}, a change-detection approach is being considered for HYDROS. Change-detection methods have been suggested in previous radar studies [42][43] [44]). The rapid global revisit every 2 to 3 days makes HYDROS ideally suited to the application of soil moisture change-detection methods (as well as for freeze/thaw state detection). This has not

been the case for previous L-band radar missions, which have had much less frequent revisit characteristics. The premise of the change-detection approach is that over short time periods, the effects on the radar signal of changes in surface roughness, topography, and vegetation cover at the HYDROS radar footprint scale are small compared to the effects of dynamic soil moisture change. Thus, change in observed backscatter during a surface wetting and drying sequence can be interpreted as due primarily to soil moisture change. The validity of this assumption is consistent with airborne observations and is being tested using SMEX02 and SMEX03 data.

A.3 Combined Radiometer and Radar Soil Moisture Retrieval

The synergy between active and passive measurements is used to enhance HYDROS retrieval capabilities. The radar retrieval algorithm derives three output quantities at 3-km resolution: soil moisture m_v, roughness h, and a Radar Vegetation Index (RVI) ($\sigma^t_{hv}/\sigma^t_{vv}$ ratio). The h and RVI are aggregated (mean and RMS) to the 40-km radiometer footprints and assimilated as inputs to the radiometric soil moisture retrieval algorithm. The 40-km passive (T_{Bp}) data are registered to an Earth-fixed grid at which the ancillary data are also pre-gridded and stored. The 40-km retrievals and output products are generated on this grid. The ancillary data and the footprint-mean RVI are used to estimate the vegetation opacity τ_c for the radiometric soil moisture retrieval. The relationships between NDVI, RVI, and opacity are derived from experimental data [32][36]. The RMS of the RVI and NDVI indices within the 40-km radiometer footprints serve as measures of surface heterogeneity. High values are indicators of possible degradation of the retrievals.

A.4 Freeze/Thaw State Retrieval from Radar Backscatter

HYDROS will provide the first capability for accurate high-resolution, high-temporal-repeat global mapping of freeze/thaw state, independent of solar illumination and cloud cover. HYDROS will utilize a radar backscatter change-detection methodology to measure the landscape freeze/thaw state. L-band backscatter response to changes in landscape freeze/thaw state is typically greater than 3 dB (Figure 4) and can be more than 5 to 7 dB [29]. This ubiquitous and unambiguous change in back-scatter dominates other temporal variations over seasonal cycles. A variety of radar back-scatter temporal change metrics have been applied for classification of frozen and thawed surface state conditions. The techniques exploit the dominance of freeze/thaw state transitions on variations of the landscape dielectric properties and associated radar backscatter variations. They include: (1) first-order difference from a reference (e.g., frozen) state; (2) fractional difference between frozen and non-frozen reference states, and (3) first order difference from a moving window mean of the temporal data stream. The HYDROS freeze/ thaw state detection algorithm will include a combination of these metrics.

B. Data Products

HYDROS ground data processing and generation of geophysical data products will be performed within the mission science and instrument teams. The data will be archived and distributed through the NASA Goddard Space Flight Center (GSFC) Distributed Active Archive Center (DAAC). Table 3 lists the principal data products from the mission.

Table 3: HYDROS Data Products

Product	**Name**
Boreal Freeze/Thaw	L3_3km_F/T
Freeze/Thaw in Carbon Exchange	L4_3km_F/T
Hydrometeorology Soil Moisture	L3_10km_SM
Hydroclimatology Soil Moisture	L3_40km_SM
Land Data Assimilation	L4_5km_4DDA

The HYDROS science team will also produce value-added data products based on land data assimilation that include estimation and their errors. This is a value-added data product that integrates HYDROS and other observations (space-borne and *in situ*) into physics-based models of land surface hydrology. The approach has the following distinct advantages:

1. Direct assimilation of brightness temperature and backscatter measurements use the synergy of active and passive sensing to produce accurate high-resolution retrievals, including measurements by sensors on board other satellites,

2. Constraining the retrieval with dynamic models of the soil-vegetation-atmosphere continuum extends the near-surface information (top 5 cm) to the root zone.

3. Estimates of moisture, energy, and carbon fluxes at the land-atmosphere boundary that are consistent with the sequences of measurements are made.

Prototypes and tests of land data assimilation systems are found in [45][46][47][48][49][50]. Additionally the product suite will include a Level 4 product linking surface freeze/thaw state to growing season timing and terrestrial carbon exchange [30][51][52].

V. Summary

This paper provides an overview of the HYDROS mission including its science rationale and objectives. It also outlines the measurement approach and instrument requirements. The HYDROS mission has been selected as a NASA ESSP pathfinder mission and it is currently in the formulation phase, with a launch date in 2010. During the formulation phase the HYDROS mission design will further undergo studies to achieve the best design that meet the maximum science objectives with reduced risk and cost. The HYDROS mission will be a core element of the NASA Earth system science focus on the water, energy, and carbon cycles. It will also bring natural hazards applications such as severe weather forecasting, flash-flood prediction, and flood and drought monitoring capabilities into a new era.

References

[1] D. Entekhabi, G. R. Asrar, A. K. Betts, K. J. Beven, R. L. Bras, C. J. Duffy, T. Dunne, R. D. Koster, D. P. Lettenmaier, D. B. McLaughlin, W. J. Shuttleworth, M. T. van Genuchten, M.-Y. Wei, E. F. Wood, "An Agenda for land-surface hydrology research and a call for the second International Hydrological Decade", *Bull. of the Am. Meteor. Soc.*, vol. 80(10), pp. 2043-2058, 1999.

[2] P. Morel, "Why GEWEX? The agenda for a global energy and water cycle research program", GEWEX News, vol. 11(1), pp. 7-11, 2001.

[3] P. A, Dirmeyer, F. J. Zeng, A. Ducharne, J. C. Morrill, and R. D. Koster, "The sensitivity of surface fluxes to soil water content in three land surface schemes", *J. of Hydrometeorology*, vol.1(2), pp. 121-134, 2000.

[4] R. D. Koster, and P. C. D. Milly, "The interplay between transpiration and runoff formulations in land surface schemes used with atmospheric models", *J. of Climate*, vol. 10(7), pp. 1578-1591, 1997.

[5] A. T. Cahill, M. B. Parlange, T. J. Jackson, P. O'Neill, T. J. Schmugge, "Evaporation from nonvegetated surfaces: Surface aridity methods and passive microwave remote sensing", *J. of Appl. Meteor.*, vol. 38(9), pp. 1346-1351, 1999.

[6] A. K. Betts, P. Viterbo, A.C.M. Beljaars, and B. J. J. M. van den Hurk, "Use of field data to diagnose land surface interaction" in *Proceedings of the ECMWF Seminar on Diagnosis of Models and Data Assimilation Systems*, September 6-10, 1999, Reading, United Kingdom, 347-364, 1999.

[7] S. Belair, L.-P. Crevier, J. Mailhot, B. Bilodeau, and Y. Delage, "Operational implementation of the ISBA land surface scheme in the Canadian regional weather forecast model. Part I: Warm season results", *J. Hydromet.*, vol. 4, pp. 352-370, 2003.

[8] J. D. Albertson, and M. B. Parlange, "Natural integration of scalar fluxes from complex terrain", *Adv. in Water Resour.*, vol. 23(3), pp. 239-252, 2000.

[9] M. L. Goulden, S. C. Wofsy, J. W. Harden, S. E. Trumbore, P. M. Crill, S. T. Gower, T. Fries, B. C. Daube, S.-M. Fan, D. J. Sutton, A. Bazzaz, and J. W. Munger, "Sensitivity of boreal forest carbon balance to soil thaw", *Science*, vol. 279(5348), pp. 214-217, 1998.

[10] S. Frolking, "Sensitivity of spruce/moss boreal forest carbon balance to seasonal anomalies in weather", *J. Geophys. Res.*, vol. 102, pp. 29,053-29,064, 1997.

[11] S. Frolking, M.L. Goulden, S.C. Wofsy, S.-M. Fan, D.J. Sutton, J.W. Munger, A.M. Bazzaz, B.C. Daube, P.M. Crill, J.D. Aber, L.E. Band, X. Wang, K. Savage, T. Moore, and R.C. Harriss, "Modelling temporal variability in the carbon balance of a spruce/moss boreal forest", *Global Change Biology*, vol. 2, pp. 343-366, 1996.

[12] J. E. Hansen, R. Ruedy, Mki. Sato, M. Imhoff, W. Lawrence, D. Easterling, T. Peterson, and T. Karl, "A closer look at United States and global surface temperature change", *J. of Geophys. Res.*, vol. 106, pp. 23947-23963, 2001.

[13] T. Zhang, T. E. Osterkamp and K. Stamnes, "Effects of climate on the active layer and permafrost on the North Slope of Alaska, U.S.A.", *Permafrost Periglacial Processes*, vol. 8(1), pp. 45-67, 1997.

[14] A. I. Shiklomanov, R. B. Lammers, and C. J. Vörösmarty, "Widespread decline in hydrological monitoring threatens panarctic research', *Eos*, vol. 83(2),pp. 16-17, 2002.

[15] E. Rignot, and J. Way, "Monitoring freeze/thaw cycles along north-south Alaskan transects using ERS-1 SAR", *Remote Sens. of the Env.*, vol. 49, pp. 131-137, 1994.

[16] L. D. Hinzman, D. L. Kane, C. S. Benson and K. R. Everett, "Energy balance and hydrological processes in an arctic watershed", In J. F. Reynolds and J. D. Tenhunen (Eds.) *Ecological Studies*, vol. 120, Springer-Verlag Berlin, pp. 131-154, 1996

[17] E. G. Njoku and D. Entekhabi, "Passive microwave remote sensing of soil moisture", *J. of Hydrology*, vol. 184(1), pp. 101-130, 1995.

[18] Y. H. Kerr and J. P. Wigneron, "Vegetation models and observations - A review" in *Passive Microwave Remote Sensing of Land-Atmosphere Interactions* (B. J. Choudhury, Y. H. Kerr, E. G. Njoku and P. Pampaloni, Eds), VSP Publishers, Utrecht, The Netherlands, 1995.

[19] T. J. Jackson, and T. J. Schmugge, "Vegetation effects on the microwave emission of soils", *Remote Sens. of the Env.*, vol. 36, pp. 203-212, 1991.

[20] T. J. Jackson, D. Chen, M. Cosh, F. Li, M. Anderson, C. Walthall, P. Doriaswamy, and E. R. Hunt, "Vegetation water content mapping using Landsat data derived normalized difference water index (NDWI) for corn and soybeans, *Remote Sens. of the Env.*, in press, 2004.

[21] R. A. M. De Jeu, M. Owe, "Further validation of a new methodology for surface moisture and vegetation optical depth retrieval", *Int. J. Remote Sensing*, vol. 24, pp. 4559-4578, 2003.

[22] J. Wen, Z. Su, Y. Ma, "Determination of land surface temperature and soil moisture from TRMM/TMI remote sensing data", *J. of Geophys. Res.*, vol. 108(D2), 10.1029/2002JD002176.

[23] J. R. Wang and B. J. Choudhury, "Remote sensing of soil moisture content over bare field at 1.4 GHz frequency", *J. of Geophys. Res.*, vol. 86, pp. 5277-5282, 1981.

[24] J. R. Wang and T. J. Schmugge, 1980: "An empirical model for the complex dielectric permittivity of soil as a function of water content", *IEEE Trans. on Geosci. and Remote Sens.*, vol. 18, pp. 288-295, 1980

[25] M. C. Dobson, F. T. Ulaby, M. T. Hallikainen, and M. A. El-Rayes, "Microwave dielectric behavior of wet soil - Part II: Dielectric mixing models, *IEEE Trans. on Geosci. and Remote Sens.*, vol. 23, pp. 35-46, 1985.

[26] F. T. Ulaby, P. C. Dubois, and J. van Zyl, "Radar mapping of surface soil moisture", *J. of Hydrology*, vol.184, pp. 57-84, 1996.

[27] J. S. Kimball, K. C. McDonald, A. R. Keyser, S. Frolking, and S. W. Running, "Application of the NASA Scatterometer (NSCAT) for determining the daily frozen and non-frozen landscape of Alaska", *Remote Sens. of the Env.*, vol. 75, pp. 113-126, 2000.

[28] S. Frolking, K. C. McDonald, J. Kimball, J. B. Way, R. Zimmermann, and S. W. Running, "Using the space-borne NASA scatterometer (NSCAT) to determine the frozen and thawed seasons of a boreal landscape", *J. of Geophys. Res.*, vol. 104 (D22), pp. 27,895-27,907, 1999.

[29] J. B. Way, R. Zimmermann, E. Rignot, K. McDonald and R. Oren, "Winter and Spring thaw as observed with imaging radar at BOREAS", *J. of Geophysic. Res.*, vol. 102(D24), pp.29673-29684, 1997.

[30] S. W. Running, J. B. Way, K. C. McDonald, J. S. Kimball, and S. Frolking "Radar remote sensing proposed for monitoring freeze/thaw transitions in boreal regions", *Eos*, vol. 80(19), pp. 213, 220-221, 1999.

[31] E. G. Njoku, W. J. Wilson, S. H. Yueh, and Y. Rahmat-Samii, "A large-antenna microwave radiometer-scatterometer concept for ocean salinity and soil moisture sensing", *IEEE Trans. on Geosci. and Remote Sens.*, vol. 38, pp. 2645-2655, 2000.

[32] T. J. Jackson, D. M. Le Vine, A. Y. Hsu, A. Oldak, P. J. Starks, C. T. Swift, J. Isham, and M. Haken, "Soil moisture mapping at regional scales using microwave radiometry: the Southern Great Plains hydrology experiment", *IEEE Trans. on Geosci. and Remote Sens.*, vol. 37, pp. 2136-2151, 1999.

[33] E. G. Njoku, and L. Li, "Retrieval of land surface parameters using passive microwave measurements at 6 to 18 GHz", *IEEE Trans. Geosci. Rem. Sens.*, vol. 37, pp. 79-93, 1999.

[34] J.-P. Wigneron, P. Waldteufel, A. Chanzy, J.-C. Calvet, and Y. Kerr,"Two-dimensional microwave interferometer retrieval capabilities over land surfaces:", *Remote Sens. of Env.*, vol. 73, pp. 270-282, 2000.

[35] Y. Oh, K. Sarabandi, and F. T. Ulaby, "An empirical model and an inversion technique for radar scattering from bare soil surface", *IEEE Trans. on Geosci. and. Remote Sens.*, vol. 30(2), pp. 370-381, 1992.

[36] P. C. Dubois, J. van Zyl, and T. Engman, "Measuring soil moisture with imaging radars, *IEEE Trans. on Geosci. and Remote Sens.*, vol. 33(4), pp. 915-926, 1995

[37] J. C. Shi, J. Wang, A. Hsu, P. O'Neill, and E. T. Engman, 1997: Estimation of bare surface soil moisture and surface roughness parameters using L-band SAR image data", *IEEE Trans. on Geosci. and Remote Sens.*, vol. 35(5), pp. 1254-1266.

[38] T. LeToan, A. Beaudoin, J. Riom, and D. Guyon, 1992: Relating forest biomass to SAR data, *IEEE Trans. on Geosci. and. Remote Sens.,* vol. 30, pp. 403-411, 1992.

[39] K. J. Ranson, G. Sun, R. Lang, N. Chauhan, R. Cacciola, and O. Kilic, "Mapping of boreal forest biomass from spaceborne synthetic aperture radar", *J. of Geophys. Res.*, vol. 102(D24), pp. 29599-29610, 1997

[40] S. Saatchi and M. Moghaddam, "Estimation of crown and stem water content and biomass of boreal forest using polarimetric

SAR imagery", *IEEE Trans. on Geosci. and Remote Sens.*, vol. 38(2), pp. 697-709, 2000.

[41] R. Bindlish and A. Barros, "Parameterization of vegetation backscatter in radar-based soil moisture estimation", *Remote Sens. of Env.*, vol. 76(1), pp. 130-137, 2001.

[42] M. C. Dobson and F. T. Ulaby, "Preliminary evaluation of the SIR-B response to soil moisture, surface roughness, and crop canopy cover", *IEEE Trans. on Geosci. and Remote Sens.*, vol. 24, pp. 517-526, 1986.

[43] A. Quesney, S. Le Hegarat-Mascle, O. Taconet, D. Vidal-Madjar, J. P. Wigneron, C. Loumagne, and M. Normand, "Estimation of watershed soil moisture index from ERS/SAR data", *Remote Sens. of Env.*, vol. 72, pp. 290-303, 2000.

[44] W. Wagner and K. Scipal "Large-scale soil moisture mapping in Western Africa using the ERS scatterometer", *IEEE Trans. on Geosci. and Remote Sens.*, vol. 38, pp. 1777-1782, 2000.

[45] P. R. Houser, W. J. Shuttleworth, J.S. Famiglietti, H.V. Gupta, K. H. Syed, and D.C. Goodrich, "Integration of soil moisture remote sensing and hydrologic modeling using data assimilation", *Water Resour. Res.*, vol. 34(12), pp. 3405-3420, 1998.

[46] D. Entekhabi, H. Nakamura and E. G. Njoku, "Solving the inverse-problem for soil moisture and temperature profiles by sequential assimilation of multifrequency remotely sensed observations", *IEEE Trans. on Geosci. and Remote Sens.*, vol. 32, pp. 438-448, 1994.

[47] J. F. Galantowicz, D. Entekhabi, and E. G. Njoku, "Tests of sequential data assimilation for retrieving profile soil moisture and temperature from observed L band radiobrightness", *IEEE Trans. on Geosci. and Remote Sens.*, vol. 37(4), pp. 1860-1870, 1998.

[48] R. Reichle, D. Entekhabi, and D. McLaughlin, "Downscaling of radiobrightness measurements for soil moisture estimation: A four-dimensional variational data assimilation approach", *Water Resour. Res.*, vol. 37(9), pp. 2353-2364, 2001.

[49] R. Reichle, D. B. McLaughlin, and D. Entekhabi, "Hydrologic data assimilation with the ensemble Kalman Filter", *Monthly Weather Rev.*, vol. 130 (1), pp. 103-114, 2002.

[50] S. A. Margulis, D. B. McLaughlin, D. Entekhabi, and S. Dunne, "Land data assimilation and estimation of soil moisture using measurements from the Southern Great Plains 1997 field experiment", *Water Resour. Res.,* vol. 38(12), doi:10.1029/2001WR001114, 2002.

[51] J. S. Kimball, K. C. McDonald, S. W. Running, and S. Frolking, 2004. "Satellite radar remote sensing of seasonal growing seasons for boreal and sub-alpine rvergreen forests," *Remote Sens. of Env.*, In Press, 2004.

[52] K. C. McDonald, J. S. Kimball, E. Njoku, R. Zimmermann, and M. Zhao, "Variability in springtime thaw in the terrestrial high latitudes: Monitoring a major control on the biospheric assimilation of atmospheric CO2 with spaceborne microwave remote sensing", *Earth Interactions.* Submitted, 2004.

Dara Entekhabi is a professor in the Department of Civil and Environmental Engineering and the Department of Earth, Atmospheric, and Planetary Sciences at the Massachusetts Institute of Technology. He is the HYDROS principal investigator.

Eni Njoku is a principal research scientist at the NASA Jet Propulsion Laboratory, California Institute of Technology. He is the HYDROS JPL Project Scientist.

Paul Houser is head of the Hydrologic Sciences Branch at the NASA Goddard Space Flight Center. He is the HYDROS GSFC Project Scientist.

Michael Spencer is a radar system engineer at the NASA Jet Propulsion Laboratory, California Institute of Technology. He is the HYDROS Instrument Manager.

Terence Doiron is a radiometer system engineer at the NASA NASA Goddard Space Flight Center. He is the HYDROS Radiometer Engineer.

Joel Smith is the HYDROS Project Manager at the NASA Jet Propulsion Laboratory, California Institute of Technology.

Ralph Girard is a senior radar engineer at the Canadian Space Agency.

Stephane Belair is a research scientist at the Meteorological Service of Canada.

Wade Crow is a research scientist at the U.S. Department of Agriculture, Agricultural Research Service - Hydrology and Remote Sensing Laboratory.

Thomas Jackson is a senior research scientist at the U.S. Department of Agriculture, Agricultural Research Service - Hydrology and Remote Sensing Laboratory.

Yann Kerr is a senior research scientist at the Centre d'Etudes Spatiales de la Biosphere, Centre National d'Etudes Spatiales.

John Kimball is a professor a the University of Montana.

Randy Koster is a research scientist at the NASA Goddard Space Flight Center.

Kyle McDonald is a research scientist at the NASA Jet Propulsion Laboratory, California Institute of Technology.

Peggy O'Neill a research scientist at the NASA Goddard Space Flight Center.

Terry Pultz is a research scientist at the Canada Centre for Remote Sensing, Natural Resources Canada.

Steve Running is a professor a the University of Montana.

J.C. Shi is a research scientist at the University of California at Santa Barbara.

Eric Wood is a professor in the Department of Civil and Environmental Engineering at Princeton University.

Jakob van Zyl is a research scientist at the NASA Jet Propulsion Laboratory, California Institute of Technology.

Table 1. HYDROS functional requirements traceability

Scientific Measurement Requirements	Instrument Functional Requirements	Spacecraft and Mission Requirements
Soil Moisture: ~±4% volumetric accuracy in top 2-5 cm for vegetation water content < 5 kg m^{-2} Hydrometeorology at ~10km Hydroclimatology at ~40km	*L-Band Radiometer:* Polarization: V, H, U; Resolution: 40 km; Relative accuracy: 1 K *L-Band Radar:* Polarization: VV, HH, HV; Resolution: 10 km; Relative accuracy: 0.5 dB for VV and HH Constant Incidence angle between 35°-50°.	Total system boresight pointing: 0.34° accuracy 0.30° stability 0.1° knowledge On-board storage of at least 3 orbits of science data S-Band downlink for radiometer and global radar (2.5 Mbps) X-Band downlink for Hi-Res radar (80 Mbps)
Freeze/Thaw State: Capture freeze/thaw transitions in integrated vegetation-soil continuum with two-day precision, at spatial scale of landscape variability (~3 km).	*L-Band Radar:* Polarization: HH; Resolution: 3 km Relative accuracy: 0.7 dB (1 dB per channel if two channels are used.) Constant incidence angle between 35°-50°.	
Sample diurnal cycle at consistent time of day (6 am / 6 pm) Global: ~3 day revisit Boreal: ~2 day revisit	Swath Width: ~ 1000 km	*Orbit:* 670 km circular polar, sun-synchronous, ~6am/6pm equator crossing
Observation over a minimum of two annual cycles	Minimum two-year mission life	Two-year baseline mission.